

DERIVATION OF STOCHASTIC ACCELERATION MODEL CHARACTERISTICS FOR SOLAR FLARES FROM *RHESSI* HARD X-RAY OBSERVATIONS

VAHÉ PETROSIAN¹ AND QINGRONG CHEN

Department of Physics, Kavli Institute for Particle Astrophysics and Cosmology, Stanford University, Stanford, CA 94305;
vahep@stanford.edu, qrchen@gmail.com

Revised manuscript submitted to ApJ Letter

ABSTRACT

The model of stochastic acceleration of particles by turbulence has been successful in explaining many observed features of solar flares. Here we demonstrate a new method to obtain the accelerated electron spectrum and important acceleration model parameters from the high resolution hard X-ray observations provided by the *Reuven Ramaty High Energy Solar Spectroscopic Imager (RHESSI)*. In our model, electrons accelerated at or very near the loop top produce thin target bremsstrahlung emission there and then escape downward producing thick target emission at the loop footpoints. Based on the electron flux spectral images obtained by the regularized inversion of the *RHESSI* count visibilities, we derive several important parameters for the acceleration model. We apply this procedure to the 2003 November 03 solar flare, which shows a loop top source up to 100–150 keV in hard X-ray with a relatively flat spectrum in addition to two footpoint sources. The results imply presence of strong scattering and a high density of turbulence energy with a steep spectrum in the acceleration region.

Subject headings: acceleration of particles — Sun: flares — Sun: X-rays, gamma rays

1. INTRODUCTION

It is well established that the impulsive phase hard X-ray (HXR) emission of solar flares is produced by bremsstrahlung of nonthermal electrons spiraling down the flare loop while losing energy primarily via elastic Coulomb collisions (Brown 1971; Hudson 1972; Petrosian 1973). Thus, HXR observations provide the most direct information on the spectrum of the radiating electrons and perhaps on the mechanism responsible for their acceleration. The common practice to extract this information has been to use the *parametric forward fitting* of HXR spectra to emission by an assumed spectrum, usually a power-law with breaks and cutoffs (or plus a thermal component), of the radiating or accelerated electrons (e.g. Holman et al. 2003). A more direct connection was established between the observations and the acceleration process first by Hamilton & Petrosian (1992), fitting to high spectral resolution but narrow band observations (Lin & Schwartz 1987), and later by Park et al. (1997), fitting to broad band observations (e.g. Marschhäuser et al. 1994; Dingus et al. 1994). This was done in the framework of stochastic acceleration (SA) by plasma waves or turbulence.

However, it is preferable to obtain the X-ray radiating electron spectrum *nonparametrically* by some inversion techniques first attempted by Johns & Lin (1992). Recently, Piana et al. (2003) and Kontar et al. (2004) applied regularized inversion techniques to obtain the radiating electron flux spectra from the spatially integrated photon spectra observed by *RHESSI* (Lin et al. 2002). This is an important advance but it gives the spectrum of the effective *radiating electrons* summed over the whole flare loop, but not the spectrum of the *accelerated electrons*. This difference arises because high spatial resolution observations, first from *Yohkoh* (Masuda et al.

1994; Petrosian et al. 2002) and now from *RHESSI* (e.g. Liu et al. 2003), have shown that, essentially for all flares, in addition to the emission from the loop footpoints (FPs) (e.g. Hoyng et al. 1981), there is substantial HXR emission from a region near the loop top (LT). Thus, the total radiating electron spectrum is a complex combination of the accelerated electrons at the LT and those present in the FPs after having been modified by transport effects.

It is therefore clear that separate inversion of the LT and FP photon spectra to electron spectra would provide more direct information on the acceleration mechanism. More recently, Piana et al. (2007) have applied the regularized inversion technique to the *RHESSI* data in the Fourier domain (Hurford et al. 2002) to obtain electron flux spectral images. The goal of this letter is to demonstrate that with the resulting spatially resolved electron flux spectra at the LT and FPs one can begin to constrain the acceleration model parameters directly.

In the next section we present a brief review of the relation between the derived electron flux images and the characteristics of the SA model and in §3 we apply this relation to a flare observed by *RHESSI*. A brief summary and our conclusion are presented in §4.

2. ACCELERATION AND RADIATION

The observations of distinct LT and FP HXR emissions, with little or no emission from the legs of the loop, point to the LT as the acceleration site and require enhanced scattering of electrons in the LT. Petrosian & Donaghy (1999) showed that the most likely scattering agent is turbulence which can also accelerate particles stochastically. In fact SA of the background thermal plasma has been the leading mechanism for acceleration of electrons (e.g. Hamilton & Petrosian 1992; Miller et al. 1996; Park et al. 1997; Petrosian & Liu 2004; Grigis & Benz 2006; Bykov & Fleishman 2009)

¹ Also Department of Applied Physics, Stanford University.

and ions (e.g. Ramaty 1979; Mason et al. 1986; Mazur et al. 1995; Liu et al. 2004, 2006; Petrosian et al. 2009), and is the most developed model in terms of comparing with observations.

2.1. Particle Kinetic Equation

In this model one assumes that turbulence is produced at or near the LT region (with background electron density n_{LT} , volume V , and size L). In presence of a sufficiently high density of turbulence the scattering can result in a mean scattering length or time (τ_{scat}) smaller than L or the crossing time ($\tau_{\text{cross}} = L/v$), leading to a nearly isotropic pitch angle distribution (Petrosian & Liu 2004). The general Fokker-Planck equation for the density spectrum $N(E)$ of the accelerated electrons, averaged over the turbulent acceleration region, simplifies to

$$\frac{\partial N}{\partial t} = \frac{\partial^2}{\partial E^2} [D_{\text{EE}}N] - \frac{\partial}{\partial E} \left[(A(E) - \dot{E}_L(E)) N \right] - \frac{N}{T_{\text{esc}}(E)} + \dot{Q}(E), \quad (1)$$

where $D_{\text{EE}}(E)$ and $A(E)$ are the diffusion rate and direct acceleration rate by turbulence², respectively, \dot{E}_L is the electron energy loss rate, and $\dot{Q}(E)$ and $N(E)/T_{\text{esc}}(E)$ describe the rate of injection of (thermal) particles and escape of the accelerated particles from the acceleration region. For electrons of energies below ~ 1 MeV, which are of interest here, Coulomb collisions³ dominate the energy loss rate,

$$\dot{E}_L = \dot{E}_{\text{Coul}} = 4\pi r_0^2 m_e c^3 n_{LT} \ln \Lambda / \beta, \quad (2)$$

where $\ln \Lambda$ is the Coulomb logarithm taken to be 20 for solar flare conditions. Following Petrosian & Liu (2004), we approximate the escape time as $T_{\text{esc}}(E) \simeq \tau_{\text{cross}}(1 + \tau_{\text{cross}}/\tau_{\text{scat}})$, which smoothly connects the two limiting cases of $\tau_{\text{cross}}/\tau_{\text{scat}} \gg 1$ and $\ll 1$. The mean scattering time is related to the pitch angle diffusion rates (Dung & Petrosian 1994; Pryadko & Petrosian 1997) due to both Coulomb collisions ($D_{\mu\mu}^{\text{Coul}}$ and $\tau_{\text{scat}}^{\text{turb}}$) and turbulence ($D_{\mu\mu}^{\text{turb}}$ and $\tau_{\text{scat}}^{\text{Coul}}$) as

$$\tau_{\text{scat}}(E) = \frac{1}{8} \int_{-1}^1 \frac{(1 - \mu^2)^2}{D_{\mu\mu}^{\text{Coul}}(\mu, E) + D_{\mu\mu}^{\text{turb}}(\mu, E)} d\mu. \quad (3)$$

Similarly we can define the scattering times $\tau_{\text{scat}}^{\text{Coul}}$ and $\tau_{\text{scat}}^{\text{turb}}$ for each process alone. For Coulomb collisions, $D_{\mu\mu}^{\text{Coul}} = \frac{2(1-\mu^2)}{\gamma+1} \frac{\dot{E}_{\text{Coul}}}{E}$. For turbulence, $D_{\mu\mu}^{\text{turb}}$, like D_{EE} , depends on the spectrum of turbulence and on the background plasma density, composition, temperature, and magnetic field (see Schlickeiser 1989; Dung & Petrosian 1994; Pryadko & Petrosian 1997, 1998, 1999; Petrosian & Liu 2004). Since these coefficients determine the spectrum of the accelerated electrons, one can then constrain some aspects of the acceleration mechanism if an accurate spectrum of the electrons can be derived from observations.

² For stochastic acceleration, $A(E) = D_{\text{EE}}\zeta(E)/E + dD_{\text{EE}}/dE$, where $\zeta(E) = (2 - \gamma^{-2})/(1 + \gamma^{-1})$, $\gamma = 1 + E/m_e c^2 = 1/\sqrt{1 - \beta^2}$ is the Lorentz factor, and $v = c\beta$ is the electron velocity.

³ At higher energies, synchrotron loss must be included in \dot{E}_L .

2.2. LT and FP Spectra

The accelerated electrons in the (LT) acceleration region with a flux spectrum $F_{\text{LT}}(E) = vN(E)$ produce *thin target* bremsstrahlung emissivity (photons $\text{s}^{-1} \text{keV}^{-1}$)

$$J_{\text{LT}}(\epsilon) = n_{\text{LT}} V \int_{\epsilon}^{\infty} F_{\text{LT}}(E) \sigma(\epsilon, E) dE, \quad (4)$$

where $\sigma(\epsilon, E)$ is the angle-averaged bremsstrahlung cross section (Koch & Motz 1959). The escaping electrons with flux $F_0(E) = N(E)L/T_{\text{esc}}$ produce *thick target* bremsstrahlung emissivity (coming mostly from the FPs) (see Petrosian 1973; Park et al. 1997),

$$J_{\text{FP}}(\epsilon) = nV \int_{\epsilon}^{\infty} F_{\text{FP}}(E) \sigma(\epsilon, E) dE, \quad (5)$$

where n is the density and F_{FP} is the effective radiating electron flux spectrum at the FPs,

$$F_{\text{FP}}(E) = vN_{\text{FP}} = \frac{v(E)}{\dot{E}_L(n)} \int_E^{\infty} \frac{N(E')}{T_{\text{esc}}(E')} dE'. \quad (6)$$

Since $\dot{E}_L \propto n$, the FP photon spectrum is independent of density. In what follows we evaluate equations (5) and (6) using the LT density n_{LT} .

2.3. Acceleration Model Parameters

Regularized inversion of *RHESSI* count visibilities gives the electron visibilities (Piana et al. 2007), which can then be used to construct images of electron flux (multiplied by column density). From these images, we extract the spatially resolved spectra, $F_{\text{LT}}(E)$ at the LT and $F_{\text{FP}}(E)$ at the FPs. Thus we can obtain the accelerated electron spectrum $N(E)$ at the thin target LT. Also from differentiation of equation (6) we derive the escape time as $T_{\text{esc}} = -N(E)/\frac{d}{dE}(F_{\text{FP}}\dot{E}_L/v)$, and by converting the denominator to a logarithm derivative we get

$$T_{\text{esc}}(E) = \frac{\tau_L(E)(F_{\text{LT}}/F_{\text{FP}})}{\delta_{\text{FP}}(E) + 2/(\gamma + \gamma^2)} \equiv \tau_L(E)\xi(E), \quad (7)$$

where the FP index $\delta_{\text{FP}}(E) = -\frac{d \ln F_{\text{FP}}}{d \ln E}$, $1/(\gamma + \gamma^2) = -\frac{d \ln v(E)}{d \ln E}$, and $\tau_L(E) = E/\dot{E}_L$ is the Coulomb loss time at the LT. The function $\xi(E)$ is an observable quantity representing the ratio T_{esc}/τ_L . In the above derivation, we have used the relativistic form of electron velocity $v(E)$.

Given $T_{\text{esc}}(E)$, from its relation to τ_{cross} and τ_{scat} , we obtain the mean scattering time as $\tau_{\text{scat}} \simeq \tau_{\text{cross}}^2/(T_{\text{esc}} - \tau_{\text{cross}})$, which is valid for $T_{\text{esc}} > \tau_{\text{cross}}$. Disentanglement of $\tau_{\text{scat}}^{\text{turb}}$ from τ_{scat} is complicated (eq. [3]) at energies when turbulence and Coulomb collisions contribute equally to τ_{scat} . However, if turbulence dominates the pitch angle diffusion, then to the first order we can write $\tau_{\text{scat}}^{\text{turb}} \simeq \tau_{\text{scat}}(1 + \tau_{\text{scat}}/\tau_{\text{scat}}^{\text{Coul}})$, and obtain some average value of $D_{\mu\mu}^{\text{turb}}$. Furthermore, given $N(E)$ we can in principle determine the other Fokker-Planck coefficients, namely $A(E)$ and D_{EE} (see eq. [1]). Therefore we can reach a consistent picture of the acceleration process due to turbulence and begin to make inroads into the spectrum and the nature of turbulence itself.

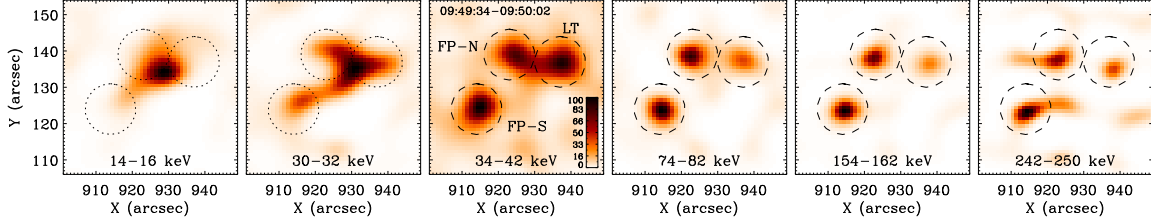


Figure 1. Electron flux spectral images (with 8 keV bin width above 34 keV and 2 keV bin width at lower energies) up to 250 keV in the 2003 November 03 flare during the nonthermal peak as reconstructed from two sets of the regularized electron visibilities by the MEM_NJIT algorithm (Schmahel et al. 2007). The images show one LT and two FP sources above 34 keV and a loop structure at lower energies. Three circles are used to extract the LT and FP electron flux spectra above 34 keV (see Figure 2).

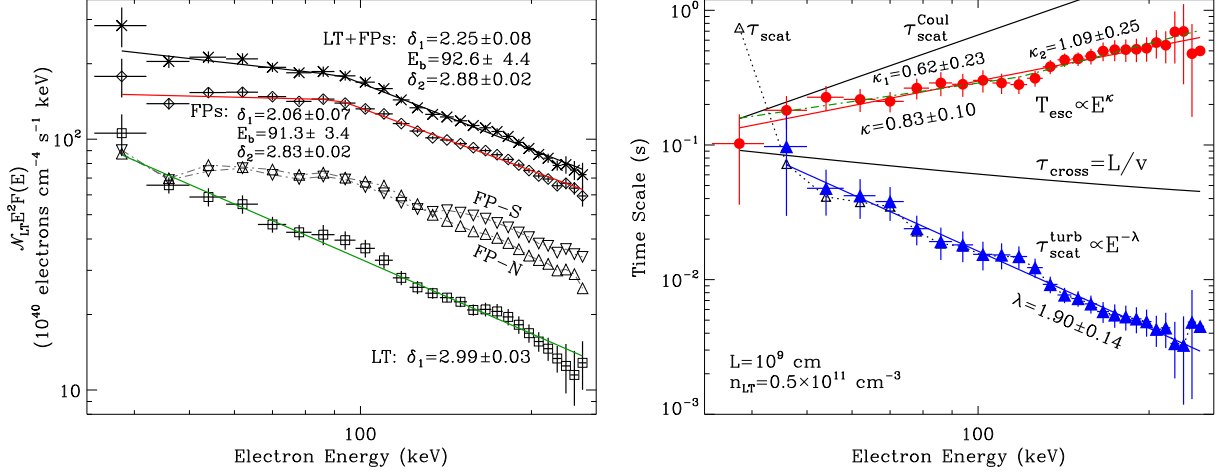


Figure 2. *Top:* Electron power spectra $\mathcal{N}_{LT} E^2 F(E)$ for the LT (*square*), the two FPs summed (*diamond*), and all three sources (LT + FPs, *cross*) in the 2003 November 03 flare. The LT spectrum can be fitted by a power-law, and the summed FP and total spectra by a broken power-law. Also note that the southern FP spectrum (*downward triangular*) is flatter than the northern FP spectrum (*upward triangular*), mostly above ~ 90 keV by ~ 0.3 powers of energy, consistent with their asymmetric locations with respect to the LT. *Bottom:* Escape time (*filled circle*) and turbulence scattering time (*filled triangular*) in the (LT) acceleration region. The escape time can be well fitted by either a power-law or a broken power-law (*dash dot*) increasing with energy, and the turbulence scattering time by a power-law rapidly decreasing with energy. Also shown are the crossing, Coulomb scattering, and the mean scattering (*open triangular*) times. The reduced chi-squares for all the fittings are below or around 1.

3. APPLICATION: THE 2003 NOVEMBER 03 FLARE

As a first demonstration, we apply our new procedure to the 2003 November 03 solar flare (X3.9 class) during the nonthermal peak, in which we find a hard LT source (extending above 100 keV in HXR) distinct from the thermal loop in addition to two FP sources⁴. In Figure 1 we show the electron flux images up to 250 keV, which also show a loop at low energies and one LT and two FPs at higher energies. In Figure 2 *top* panel we show the electron spectra $\mathcal{N}_{LT} E^2 F(E)$, where $\mathcal{N}_{LT} = n_{LT} L$ is the LT column density. The LT flux spectrum can be fitted by a power-law with an index $\delta_{LT} = 3.0$. The summed FP flux spectrum can be better fitted by a broken power-law with the indexes $\delta_1 = 2.1$ and $\delta_2 = 2.8$ below and above the break energy $E_b = 91 \pm 3$ keV. It is clear that the total radiating electron spectrum differs significantly from the (LT) accelerated electron spectrum.

Given the above LT and FP electron flux spectra we derive the energy dependence of the escape time (eq. [7]). The LT density can be estimated as $n_{LT} \simeq \sqrt{EM/L^3} \simeq 0.5 \times 10^{11} \text{ cm}^{-3}$, where the LT size $L \simeq 10^9 \text{ cm}$ is obtained from the LT angular size, and the emission mea-

sure EM $\simeq 0.2 \times 10^{49} \text{ cm}^{-3}$ is obtained from spectral fitting of the LT thermal emission. As in Figure 2 *bottom* panel, the escape time increases slowly with energy and can be fitted by either a power-law,

$$T_{\text{esc}}(E) = 0.3 \text{ s} \left(\frac{E}{100 \text{ keV}} \right)^{\kappa}, \quad \kappa = 0.83 \pm 0.10, \quad (8)$$

or a broken power-law with a break at $E_b = 118 \pm 37$ keV, and the indexes $\kappa_1 = 0.62 \pm 0.23$ and $\kappa_2 = 1.09 \pm 0.25$. The fact that the escape time should be longer than the crossing time yields an upper limit on \mathcal{N}_{LT} , which is satisfied by the above LT density and size.

We then calculate the mean scattering time in the LT region. Except at the lowest energy, the Coulomb contribution is small so that the scattering time thus calculated can be attributed to turbulence. The scattering time due to turbulence (see §2.3) can be fitted by a power-law above ~ 40 keV,

$$\tau_{\text{scat}}^{\text{turb}} = 0.016 \text{ s} \left(\frac{E}{100 \text{ keV}} \right)^{-\lambda}, \quad \lambda = 1.90 \pm 0.14. \quad (9)$$

4. SUMMARY AND DISCUSSION

In this paper we describe a new method to directly obtain the model parameters for stochastic acceleration

⁴ Q. Chen & V. Petrosian (2010a, in preparation) present HXR observations of this flare and argue that the high energy LT source should not be an artifact of the pulse pileup effect.

of particles by turbulence in solar flares from regularized inversion of the high resolution *RHESSI* HXR data (Piana et al. 2007). We have argued that particle acceleration takes place at or near the LT region. The accelerated electrons produce thin target emission at the LT and then escape downward to the dense FP region undergoing Coulomb collisions and producing thick target emission. In this model the LT and FP electron spectra are connected by the escape process from the LT region (eq. [6]), thus allowing us to determine the energy dependence of the escape time. Our method has the advantage that one can now constrain the model parameters uniquely rather than just satisfying the consistency between the model and the data as commonly done by forward fitting routines. This method can be applied to flares with simultaneous HXR emission from the LT and FP sources.

We have applied our method to the 2003 November 03 flare, in which we can obtain the electron flux images for both the LT and FPs up to 250 keV. The LT accelerated electron flux spectrum can be fitted by a power-law and the effective radiating flux spectrum at the FPs is better fitted by a broken power-law. From these spectra we derive the energy variation of the escape time and the scattering time. As seen in Figure 2, the turbulence scattering time is relatively short and decreases with energy. A short scattering time may arise from a high energy density of turbulence ($\mathcal{E}_{\text{turb}}$), with the exact relationship depending also on the magnetic field (B), and the spectral index (q) and minimum wave number (k_{min}) of turbulence. A high level of turbulence also implies efficient acceleration which generally means a flat spectrum for the accelerated electrons, which is the case for the current flare. The energy dependences of $\tau_{\text{scat}}^{\text{turb}}$ and D_{EE} are also a function of these characteristics of turbulence; at high energies they are determined primarily by the spectral index of turbulence (see Dung & Petrosian 1994; Pryadko & Petrosian 1997, 1998, 1999; Liu et al. 2006).

For the usually assumed Kolmogorov ($q = 5/3$) or Iroshnikov-Kraichnan ($q = 3/2$) turbulence spectra, one expects the scattering time to increase with energy as E^{2-q} , which translates into an escape time varying roughly as $T_{\text{esc}} \propto 1/\sqrt{E}$ at high (but non-relativistic) energies. The energy dependences of T_{esc} and $\tau_{\text{scat}}^{\text{turb}}$ obtained here require a steeper turbulence spectrum ($q > 3$) at high wave numbers. Such a steep spectrum can be present beyond the inertial range where damping is important (e.g. Jiang et al. 2009). The electron energies and the wave-particle resonance condition determine the wave vector of the accelerating plasma waves. This relation depends primarily on the plasma parameter $\alpha \propto \sqrt{n}/B$ (e.g. Petrosian & Liu 2004). Thus, given the magnetic field and plasma density we can determine the wave vectors for transition from the inertial to the damping ranges of turbulence.

It should, however, be emphasized that the results obtained here may not be representative of typical flares. More commonly flares have much softer LT emission, which would give an escape time decreasing (and scattering time increasing) with energy, consistent with a low level and a flat spectrum of turbulence.

The exact relation between the derived quantities ($N(E)$, T_{esc} , and $\tau_{\text{scat}}^{\text{turb}}$) and the turbulence character-

istics ($\mathcal{E}_{\text{turb}}, B, q$, etc.) is complicated and depends on the angle of propagation of the plasma waves with respect to magnetic field and other plasma conditions. In future, we will apply these procedures to more flares (Q. Chen & V. Petrosian, 2010b, in preparation) and deal with these relations explicitly.

We thank the referee for helpful comments. We thank Anna Maria Massone and Gordon Hurford for providing the visibility inversion code and valuable discussions about data analysis, and Siming Liu and Wei Liu for various discussions. *RHESSI* is a NASA small explorer mission. This work is supported by NSF grant ATM0648750 and NASA grant NNX10AC06G.

REFERENCES

- Brown, J. C. 1971, *Sol. Phys.*, 18, 489
 Bykov, A. M., & Fleishman, G. D. 2009, *ApJ*, 692, L45
 Dingus, B. L., et al. 1994, in *AIP Conf. Proc.* 294, High-energy Solar Phenomena, ed. J. M. Ryan & W. T. Vestrand (New York: AIP), 177
 Dung, R., & Petrosian, V. 1994, *ApJ*, 421, 550
 Grigis, P. C., & Benz, A. O. 2006, *A&A*, 458, 641
 Hamilton, R. J., & Petrosian, V. 1992, *ApJ*, 398, 350
 Holman, G. D., Sui, L., Schwartz, R. A., & Emslie, A. G. 2003, *ApJ*, 595, L97
 Hoyng, P., et al. 1981, *ApJ*, 246, L155
 Hudson, H. S. 1972, *Sol. Phys.*, 24, 414
 Hurford, G. J., et al. 2002, *Sol. Phys.*, 210, 61
 Jiang, Y. W., Liu, S., & Petrosian, V. 2009, *ApJ*, 698, 163
 Johns, C. M., & Lin, R. P. 1992, *Vol. Phys.*, 137, 121
 Koch, H. W., & Motz, J. W. 1959, *Rev. Mod. Phys.*, 31, 920
 Kontar, E. P., Piana, M., Massone, A. M., Emslie, A. G., & Brown, J. C. 2004, *Sol. Phys.*, 225, 293
 Lin, R. P., & Schwartz, R. A. 1987, *ApJ*, 312, 462
 Lin, R. P., et al. 2002, *Sol. Phys.*, 210, 3
 Liu, S., Petrosian, V., & Mason, G. M. 2004, *ApJ*, 613, L81
 Liu, S., Petrosian, V., & Mason, G. M. 2006, *ApJ*, 636, 462
 Liu, W., Jiang, Y. W., Petrosian, V., & Metcalf, T. R. 2003, *Bulletin of the American Astronomical Society*, 35, 839
 Marschhäuser, H., Rieger, E., & Kanbach, G. 1994, in *AIP Conf. Proc.* 294, High-energy Solar Phenomena, ed. J. M. Ryan & W. T. Vestrand (New York: AIP), 171
 Mason, G. M., Reames, D. V., von Rosenvinge, T. T., Klecker, B., & Hovestadt, D. 1986, *ApJ*, 303, 849
 Masuda, S., Kosugi, T., Hara, H., Tsuneta, S., & Ogawara, Y. 1994, *Nature*, 371, 495
 Mazur, J. E., Mason, G. M., & Klecker, B. 1995, *ApJ*, 448, L53
 Miller, J. A., Larosa, T. N., & Moore, R. L. 1996, *ApJ*, 461, 445
 Park, B. T., Petrosian, V., & Schwartz, R. A. 1997, *ApJ*, 489, 358
 Petrosian, V. 1973, *ApJ*, 186, 291
 Petrosian, V., & Donaghy, T. Q. 1999, *ApJ*, 527, 945
 Petrosian, V., Donaghy, T. Q., & McTiernan, J. M. 2002, *ApJ*, 569, 459
 Petrosian, V., Jiang, Y. W., Liu, S., Ho, G. C., & Mason, G. M. 2009, *ApJ*, 701, 1
 Petrosian, V., & Liu, S. 2004, *ApJ*, 610, 550
 Piana, M., Massone, A. M., Hurford, G. J., Prato, M., Emslie, A. G., Kontar, E. P., & Schwartz, R. A. 2007, *ApJ*, 665, 846
 Piana, M., Massone, A. M., Kontar, E. P., Emslie, A. G., Brown, J. C., & Schwartz, R. A. 2003, *ApJ*, 595, L127
 Pryadko, J. M., & Petrosian, V. 1997, *ApJ*, 482, 774
 Pryadko, J. M., & Petrosian, V. 1998, *ApJ*, 495, 377
 Pryadko, J. M., & Petrosian, V. 1999, *ApJ*, 515, 873
 Ramaty, R. 1979, in *AIP Conf. Proc.* 56, Particle Acceleration Mechanisms in Astrophysics, ed. J. Arons, C. McKee, & C. Max (New York: AIP), 135
 Schlickeiser, R. 1989, *ApJ*, 336, 243
 Schmahl, E. J., Pernak, R. L., Hurford, G. J., Lee, J., & Bong, S. 2007, *Sol. Phys.*, 240, 241